Critical Density for Connectivity in 2D and 3D Wireless Multi-Hop Networks

Seh Chun Ng, *Member, IEEE,* Guoqiang Mao, *Senior Member, IEEE,*
and Brian D. O. Anderson, *Life Fellow, IEEE*

***Abstract*—In this paper we investigate the critical node density required to ensure that an arbitrary node in a large-scale wireless multi-hop network is connected (via multi-hop path) to infinitely many other nodes with a positive probability. Specifically we consider a wireless multi-hop network where nodes are distributed in $\mathbb{R}^d$ $(d = 2, 3)$ following a homogeneous Poisson point process. The establishment of a direct connection between any two nodes is independent of connections between other pairs of nodes and its probability satisfies some intuitively reasonable conditions, viz. rotational and translational invariance, non-increasing monotonicity, and integral boundedness. Under the above random connection model we first obtain analytically the upper and lower bounds for the critical density. Then we compare the new bounds with other existing bounds in the literature under the unit disk model and the log-normal model which are special cases of the random connection model. The comparison shows that our bounds are either close to or tighter than the known ones. To the best of our knowledge, this is the first result for the random connection model in both 2D and 3D networks. The result is of practical use for designing large-scale wireless multi-hop networks such as wireless sensor networks.**

***Index Terms*—Random geometric graph, critical density, Poisson random connection model, continuum percolation.**

I. Introduction

CONNECTIVITY is a fundamental property of large-scale wireless multi-hop networks and has been actively studied in recent years. One of the best known results on the connectivity of large-scale wireless multi-hop networks is by Gupta and Kumar [1]. Given n nodes independently, identically and uniformly distributed in a unit disk area in $\mathbb{R}^2$, and under the assumption that the communication between nodes follows the unit disk communication model, they investigated the critical transmission range required so that every node in a network is asymptotically connected to every other node as n goes to infinity. However, as shown in [2], [3], requiring all nodes of a wireless multi-hop network to be inter-connected results in a poor scalability of the network transport capacity. In contrast, Dousse et al. [4], [5] showed that it is no longer the case if we only slightly loosen the connectivity requirement, by demanding that most nodes be connected to each other. More specifically, by allowing an arbitrarily small (albeit constant) fraction of nodes to be disconnected, they showed that the per-node throughput remains constant as the network size increases. In addition, a network which tolerates a small fraction of nodes to be disconnected requires much lower transmission range / power than a network which requires all nodes to be inter-connected [6], [7]. Reducing transmission power is particularly beneficial for wireless sensor networks as sensors are normally battery-operated and hard to replace when they fail. From the application point of view, it is often acceptable for a wireless sensor network with a large number of redundant sensors to have a small number of sensors disconnected. A sensor network is considered to be functional as long as it is able to collect information from almost the entire sensing area (see [8], [9], [10] for related sensing coverage problems). Therefore, a widely studied connectivity problem of large-scale networks is the node density required to ensure the existence of some long distance multi-hop paths in the network so that each node can possibly communicate with a large number of other nodes in the network (e.g. see [11], [12]). This problem is tightly related to the well-known critical density problem in continuum percolation. Other work in the area [13], [14], [15], [16], [3], [5] focuses on analyzing the capacity and latency of large-scale wireless multi-hop network when long distance multi-hop paths exist, i.e. the network percolates, and are used to transfer packets across the network. The concepts of continuum percolation theory fit well in this type of study.

In this paper the same approach is followed, i.e. we study the connectivity of large-scale wireless multi-hop networks from percolation perspective. Specifically, we consider wireless multi-hop network where nodes are distributed in $\mathbb{R}^d$ $(d = 2, 3)$ following a homogeneous Poisson point process with known and finite density λ. A random connection model with the connection function $\bar{g} : \mathbb{R}^+ \to [0, 1]$ is used to model the establishment of direct connections between

Manuscript received November 30, 2011; revised June 14 and October 28; accepted January 8, 2013. The associate editor coordinating the review of this paper and approving it for publication was S. Shakkottai.

S. C. Ng and G. Mao are with the School of Electrical and Information Engineering, The University of Sydney, Australia, and National ICT Australia (NICTA), Sydney (e-mail: {seh.ng, guoqiang.mao}@sydney.edu.au).

B. D. O. Anderson is with the Research School of Engineering, The Australian National University, Australia, and National ICT Australia (NICTA), Canberra (e-mail: brian.anderson@anu.edu.au).

This work is partially supported by the ARC (Australian Research Council) Discovery Project DP110100538, ARC Discovery Project DP120102030, and by National ICT Australia (NICTA), which is funded by the Australian Government through the Department of Broadband, Communications and the Digital Economy and the Australian Research Council through the ICT Centre of Excellence program.

This material is based on research partially sponsored by the Air Force Research Laboratory, under agreement number FA2386-10-1-4102. The U.S. Government is authorized to reproduce and distribute reprints for Governmental purposes notwithstanding any copyright notation thereon. The views and conclusions contained herein are those of the authors and should not be interpreted as necessarily representing the official policies or endorsements, either expressed or implied, of the Air Force Research Laboratory or the U.S. Government.

Digital Object Identifier 10.1109/TWC.2013.13.112130

nodes. In the model, two nodes located at $\mathbf{x} \in \mathbb{R}^d$ and $\mathbf{y} \in \mathbb{R}^d$ respectively are directly connected with probability $\bar{g}(\|\mathbf{x}-\mathbf{y}\|)$, independent of other pairs of nodes, where $\|.\|$ is the Euclidean norm. The connection function $\bar{g}$ satisfies the following properties of rotational and translational invariance, non-increasing monotonicity, and integral boundedness [17], [18]:

$$\begin{cases} \bar{g}(x) = \bar{g}(y) & \text{whenever } x = y, \\ \bar{g}(x) \leq \bar{g}(y) & \text{whenever } x \geq y, \\ 0 < \int_{\mathbb{R}^d} \bar{g}(\|\mathbf{x}\|) d\mathbf{x} < \infty. \end{cases} \quad (1)$$

It is shown that under the above model there exists a critical density above which an arbitrarily chosen node is connected to an infinite number of other nodes via multi-hop paths with a positive probability, and below which the node is almost surely connected to finite number of other nodes only [17, p. 152].

It has been shown in the literature that the exact value of critical density is hard to obtain analytically [19], [20], [21], [22]. In addition, numerical estimation of the critical density does not provide a closed-form formula and hence cannot offer better insight and intuition behind the interactions of various performance-impacting parameters. Therefore, in this paper we obtain analytically an upper and a lower bound for the critical density. The lower bound (Theorem 2) for the critical density is obtained using a Galton-Watson branching process [18] and the upper bound (Theorem 4 and 5) is obtained by relating the problem to that of site percolation on a lattice [23]. We then consider two special cases of the random connection model, viz. the unit disk communication model and the log-normal shadowing model, and obtain specific bounds under both models.

- In the unit disk model, two nodes are directly connected if and only if their Euclidean distance x is less than or equal to the transmission range r. That is, for $x \in \mathbb{R}^+$,

$$\bar{g}(x) = \begin{cases} 1 & \text{if } x \leq r, \\ 0 & \text{otherwise.} \end{cases} \quad (2)$$

- In the log-normal model, two nodes separated by a Euclidean distance x are directly connected with probability

$$\bar{g}(x) = Q(\frac{10\alpha}{\sigma} \log_{10} \frac{x}{r}) \quad (3)$$

for $x \in \mathbb{R}^+$ where $Q(y) = \frac{1}{\sqrt{2\pi}} \int_y^\infty \exp(-\frac{z^2}{2}) dz$ is the tail probability of the standard normal distribution, α is the path loss exponent, σ^2 is the shadowing variance, r is the transmission range ignoring shadowing effect. Refer to [24] for more details about the log-normal model. Note that the log-normal model (Eq. (3)) reduces to the unit disk model (Eq. (2)) when $\sigma = 0$.

Note that the unit disk model is normally adopted as a first-order approximation of communication by isotropic radiating radio signals [18]. On the other hand, the log-normal model takes into account the shadowing effect caused by the surrounding environment [25]. The model has been confirmed empirically to accurately capture the variation in received signal power in both outdoor and indoor radio propagation environments (see [26] and the references therein).

As will be further discussed in the next section, some studies related to the bounds for the critical density under different connection models can be found in the literature [17], [18], [27], [28], [19], [29]. Compared to those studies, our major contributions can be summarized as follows:

- We provide rigorous and reasonably tight upper and lower bounds for the critical density in $\mathbb{R}^2$ and $\mathbb{R}^3$ under the random connection model, with the log-normal model and the unit disk model being its two special cases.
- To the best of our knowledge, it is for the first time that a lower bound in $\mathbb{R}^2$ and $\mathbb{R}^3$ under the log-normal model is provided; furthermore, our upper bound is also tighter than the one obtained by Li and Yang [29] in $\mathbb{R}^2$ under the log-normal model.
- Our upper and lower bounds in $\mathbb{R}^2$ under the unit disk model are as tight as the widely known bounds obtained by Meester and Roy [17, p. 85], and close to the bounds obtained in [27], [28], [19].
- In real world scenarios, the direct connection between a pair of wireless nodes is affected by many factors, including shadow fading or multi-path fading [25, p. 106]. The random connection model takes into account channel randomness; hence it suits a broader class of real world situations. As the random connection model is used in this paper, the contribution of this work is non-negligible.

Further comparisons between our work and [17], [27], [28], [19], [29] are included in Section IV and V. In this paper, we do not consider the impact of interference to connectivity. The impact of interference can be managed for a network with low to moderate traffic load by carefully scheduling transmissions in the network. Furthermore, an upper bound for interference experienced by any node in a network can be obtained under some scheduling schemes (e.g. see [30]). The upper bound can then be used to generalize results obtained under the unit disk model to one considering interference.

The rest of this paper is organized as follows. In Section II we introduce related work on the critical density. In Section III we define the Poisson random connection model and the notations to be used later in the paper. We obtain analytically a lower bound for the critical density in the Poisson random connection model in Section IV. Then in the same section we compare our results with other existing results in the literature under the unit disk model and the log-normal model. Similarly, in Section V we include the analysis and discussion for the upper bound. Finally conclusions and future work are given in Section VI.

II. Related Work

Some bounds for the critical density have been given in the literature, but almost exclusively for the unit disk model. To the best of our knowledge, there is no tight and rigorous bound reported for the random connection model. The existing studies on the critical density under the random connection model mainly focus on proving that the critical density is positive and finite. To complete the proof, a lower bound which is larger than zero and an upper bound which is smaller than infinity are constructed. However, these bounds are usually loose (e.g. see [18, p. 38]).

Most results [17], [27], [28], [19] were obtained under the unit disk model in the literature, especially in $\mathbb{R}^2$. Since the results in $\mathbb{R}^2$ were obtained with different transmission ranges, we rescale the results using the scaling law [17, p. 30] to a common transmission range of 2, and report them as follows: A well-known set of analytical lower and upper bounds for the critical density was given by Meester and Roy [17], i.e. the critical density should lie between 0.174 and 0.843. Philips et al. [27] obtained a same lower bound as in [17] but a slightly tighter upper bound (0.8376). On the other hand, Gu and Hong [28] reported the same upper bound as in [17] but a tighter lower bound (0.2553). Kong and Yeh [19] obtained another lower bound (0.1925) for the critical density. No upper bound was obtained in [19]. Note that a lower bound in $\mathbb{R}^3$ under the unit disk model is also reported in [19].

Some limited work was reported under connection models other than the unit disk model. In [20], Kong and Yeh extended the unit disk model to a unit disk model with unreliable links. In the new model, two nodes are no longer directly connected with probability 1 but with some lesser probability, provided their Euclidean distance is within the transmission range r. The lower bound obtained is comparable with their earlier result obtained under the normal unit disk model [19]. In $\mathbb{R}^2$ and under the log-normal model, Li and Yang [29] obtained analytically an upper bound for the critical density. Note that the connection models used in [20] and [29] are special cases of the random connection model considered in this paper.

III. Definitions and Notations

In this section we include definitions and notations to be used later in the paper. First we formally define the Poisson random connection model which is used in this paper to model large-scale wireless multi-hop networks and the connections between nodes.

Definition 1. Let $\mathcal{H}_\lambda^d$ denote a homogeneous Poisson process of density λ on the d-dimensional Euclidean space $\mathbb{R}^d$. Let $\mathcal{H}_{\lambda,\mathbf{x_0}}^d$ denote the point process $\mathcal{H}_\lambda^d$ with an additional node at $\mathbf{x_0} \in \mathbb{R}^d$. Then the Poisson random connection model $G(\mathcal{H}_{\lambda,\mathbf{x_0}}^d; \bar{g})$ represents a random network with node set $\mathcal{H}_{\lambda,\mathbf{x_0}}^d$. Any two nodes (with coordinates $\mathbf{x}$ and $\mathbf{y}$ respectively) are directly connected with probability $\bar{g}(\|\mathbf{x}-\mathbf{y}\|)$, independent of the connections between other pairs of nodes, where function $\bar{g}$ satisfies properties in (1).

In this paper, we consider specifically $d = 2, 3$. Next, we define the percolation probability [18].

Definition 2. Let $\mathcal{W}$ be the set of nodes in $G(\mathcal{H}_{\lambda,\mathbf{x_0}}^d; \bar{g})$ connected (by multi-hop paths) to the node at $\mathbf{x_0}$. Denote by $|\mathcal{W}|$ the number of nodes in $\mathcal{W}$. Then the percolation probability $\theta(\lambda) = \Pr\{|\mathcal{W}| = \infty\}$ is the probability that $\mathcal{W}$ contains an infinite number of nodes.

The fact that the location of the chosen node in the definition of $\mathcal{W}$ is specified to be at $\mathbf{x_0} \in \mathbb{R}^d$ is of no importance: due to the stationarity property of a Poisson point process, the node can be anywhere in $\mathbb{R}^d$. Also as pointed out by the Palm theory [31] on the other hand, assuming a node at $\mathbf{x_0}$ does not prevent the distribution of the rest of the nodes to be maintained the same as $\mathcal{H}_\lambda^d$. Evidently from Definition 2, $\theta(\lambda) > 0$ means that an arbitrarily chosen node is connected to an infinite number of nodes with a positive probability. It can be shown that $\theta(\lambda)$ displays the following phase transition phenomenon for $d = 2, 3$.

Theorem 1 (Theorem 6.1 in [17])**.** *For $G(\mathcal{H}_{\lambda,\mathbf{x_0}}^d; \bar{g})$ with $d = 2, 3$, there exists a critical density $0 < \lambda_c < \infty$ such that $\theta(\lambda) = 0$ for $\lambda < \lambda_c$ and $\theta(\lambda) > 0$ for $\lambda > \lambda_c$.*

IV. Lower Bound for λ_c

A. Analysis

For convenience in later discussion, define the connection function alternatively, via a function $g : \mathbb{R}^d \to [0, 1]$ such that $g(\mathbf{x}) = \bar{g}(\|\mathbf{x}\|)$ for any $\mathbf{x} \in \mathbb{R}^d$ ($d = 2, 3$).

The following lemma is used in obtaining the lower bound for λ_c.

Lemma 1. *Consider $G(\mathcal{H}_{\lambda,\mathbf{x_0}}^d; \bar{g})$ for $d = 2, 3$ and denote by X_0 the node at $\mathbf{x_0}$. A node $Y \in \mathcal{H}_\lambda^d$ is called a k-hop node if the length of the shortest path between Y and X_0, measured by the number of hops, is k. Let N_k be the total number of k-hop nodes. Then for all k, $E[N_k]$ is finite, with*

$$E[N_1] = \int_{\mathbb{R}^d} \lambda g(\mathbf{y}-\mathbf{x_0}) d\mathbf{y} \triangleq \int_{\mathbb{R}^d}\int_{\mathbb{R}^d} h_1(\mathbf{y},\mathbf{z}) d\mathbf{z} d\mathbf{y} \quad (4)$$

where

$$h_1(\mathbf{y},\mathbf{z}) = \lambda g(\mathbf{y}-\mathbf{z})\phi(\mathbf{z}-\mathbf{x_0}), \quad (5)$$

$\phi(.)$ is the Dirac delta function; and

$$E[N_k] \le \int_{\mathbb{R}^d}\int_{\mathbb{R}^d} h_k(\mathbf{y},\mathbf{z}) d\mathbf{z} d\mathbf{y} \quad (6)$$

for $k \ge 2$ where

$$h_k(\mathbf{y},\mathbf{z}) = \int_{\mathbb{R}^d} \lambda g(\mathbf{y}-\mathbf{z})[1-g(\mathbf{y}-\mathbf{w})] h_{k-1}(\mathbf{z},\mathbf{w}) d\mathbf{w}. \quad (7)$$

Proof: This proof consists of two parts. First we derive Eq. (4) and (6), then we prove that $E[N_k]$ is finite. The derivations of Eq. (4) and (6) is based on the use of Galton-Watson branching process. Particularly, the k-hop nodes can be imagined as the members of k-th generation in the Galton-Watson branching process, while seeing node X_0 as the root of the branching process. The distribution of the k-hop nodes is then obtained by considering the impact from the previous two hops nodes, i.e. $(k-1)$-hop nodes and $(k-2)$-hop nodes. Using this approach, the expected number of 1-hop nodes (Eq. (4)) and an upper bound of the expected number of k-hop nodes (Eq. (6) for $k \ge 2$) are then derived. The detailed derivations are explained in the next few paragraphs.

Imagine we partition the $\mathbb{R}^d$ space ($d = 2, 3$) into small and non-overlapping d-cubes of side length Δ. Assume that one of the d-cubes is centered at $\mathbf{x_0}$. Then we have a collection of d-cubes centered at $\mathbb{D}^d = \{\mathbf{x_0} + (\mathbf{v}\cdot\Delta) : \mathbf{v} \in \mathbb{Z}^d\}$. Denote by $B_\mathbf{x}$ the d-cube centered at $\mathbf{x}$. The Lebesgue measure of $B_\mathbf{x}$ is $\delta\mathbf{x} \triangleq |B_\mathbf{x}| = \Delta^d$. Since nodes are Poissonly distributed in $\mathbb{R}^d$, for a sufficiently small Δ the probability that there exists exactly one node within $B_\mathbf{x}$ is $p_1(B_\mathbf{x}) = \lambda\delta\mathbf{x} + o(\delta\mathbf{x})$ where $o(\delta\mathbf{x})$ denotes a quantity which, for small $\delta\mathbf{x}$, is of lower order than $\delta\mathbf{x}$, i.e. $\lim_{\delta\mathbf{x}\to 0} \frac{o(\delta\mathbf{x})}{\delta\mathbf{x}} = 0$. The probability that there is

more than one node in $B_{\mathbf{x}}$ is $o(\delta\mathbf{x})$. Let $I_{\mathbf{x}}^k$ be the indicator random variable of the event that there exists exactly one node within the d-cube $B_{\mathbf{x}}$ *and* the node is a k-hop node. By the monotone convergence theorem, we have that

$$E[N_k] = \lim_{\Delta\to 0} \sum_{\mathbf{x}\in\mathbb{D}^d\setminus\{\mathbf{x_0}\}} E\left[I_{\mathbf{x}}^k\right] = \lim_{\Delta\to 0} \sum_{\mathbf{x}\in\mathbb{D}^d\setminus\{\mathbf{x_0}\}} \Pr\left\{I_{\mathbf{x}}^k = 1\right\} \quad (8)$$

and the limit exists. Similarly, let $J_{\mathbf{x}}$ be the indicator random variable of the event that there exists exactly one node within $B_{\mathbf{x}}$. Without loss of generality, we assume that when $J_{\mathbf{x}} = 1$ or $I_{\mathbf{x}}^k = 1$, the node within $B_{\mathbf{x}}$ is located at $\mathbf{x}$. The difference between the actual location of the node within $B_{\mathbf{x}}$ and $\mathbf{x}$ becomes negligibly small as $\Delta \to 0$. Let $H_{\mathbf{x},\mathbf{y}}$ be the indicator random variable of the event that a node at $\mathbf{x}$ and another node at $\mathbf{y}$ are directly connected.

The probability that a 1-hop node exists in $B_{\mathbf{y}}$ is

$$\begin{aligned}\Pr\left\{I_{\mathbf{y}}^1 = 1\right\} &= \Pr\left\{J_{\mathbf{y}} = 1, H_{\mathbf{y},\mathbf{x_0}} = 1\right\} \\ &= g(\mathbf{y}-\mathbf{x_0}) \times [\lambda\delta\mathbf{y} + o(\delta\mathbf{y})]. \end{aligned} \quad (9)$$

Using Eq. (8) and (9) we obtain

$$E[N_1] = \lim_{\Delta\to 0} \sum_{\mathbf{y}\in\mathbb{D}^d\setminus\{\mathbf{x_0}\}} \Pr\left\{I_{\mathbf{y}}^1 = 1\right\} = \int_{\mathbb{R}^d} \lambda g(\mathbf{y}-\mathbf{x_0}) d\mathbf{y} \quad (10)$$

which is Eq. (4).

A node is a 2-hop node if it is directly connected to *at least* one of the 1-hop nodes but not directly connected to the node at $\mathbf{x_0}$. By applying the union bound and with some arithmetic steps we obtain

$$\begin{aligned} E[N_2] &= \lim_{\Delta\to 0} \sum_{\mathbf{y}\in\mathbb{D}^d\setminus\{\mathbf{x_0}\}} \Pr\left\{I_{\mathbf{y}}^2 = 1\right\} \\ &\le \lim_{\Delta\to 0} \sum_{\mathbf{y}\in\mathbb{D}^d\setminus\{\mathbf{x_0}\}} \sum_{\mathbf{z}\in\mathbb{D}^d\setminus\{\mathbf{y},\mathbf{x_0}\}} \Big[\Pr\left\{I_{\mathbf{z}}^1 = 1\right\} \\ &\quad \times \Pr\left\{J_{\mathbf{y}} = 1, H_{\mathbf{y},\mathbf{z}} = 1, H_{\mathbf{y},\mathbf{x_0}} = 0 \middle| I_{\mathbf{z}}^1 = 1\right\}\Big] \\ &\qquad\qquad \text{[see Appendix A]} \quad (11) \\ &= \lim_{\Delta\to 0} \sum_{\mathbf{y}\in\mathbb{D}^d\setminus\{\mathbf{x_0}\}} \sum_{\mathbf{z}\in\mathbb{D}^d\setminus\{\mathbf{y},\mathbf{x_0}\}} [g(\mathbf{z}-\mathbf{x_0})[\lambda\delta\mathbf{z} + o(\delta\mathbf{z})] \\ &\quad \times g(\mathbf{y}-\mathbf{z})[1-g(\mathbf{y}-\mathbf{x_0})][\lambda\delta\mathbf{y} + o(\delta\mathbf{y})]] \\ &= \int_{\mathbb{R}^d}\int_{\mathbb{R}^d} \lambda^2 g(\mathbf{y}-\mathbf{z})[1-g(\mathbf{y}-\mathbf{x_0})] g(\mathbf{z}-\mathbf{x_0}) d\mathbf{z}d\mathbf{y} \quad (12) \end{aligned}$$

and hence Eq. (6) is proved for $k = 2$.

From Eq. (5), we have $h_1(\mathbf{y},\mathbf{z})$ defined as the probability that the node at $\mathbf{y}$ is directly connected to the node at $\mathbf{x_0}$. That is, the node at $\mathbf{y}$ is a 1-hop node. Applying Eq. (5) into Eq. (7), it can be shown that $h_2(\mathbf{y},\mathbf{z})$ is the probability that the node at $\mathbf{y}$ is directly connected to the 1-hop node at $\mathbf{z}$ but not directly connected to the node at $\mathbf{x_0}$. That is, the node at $\mathbf{y}$ is a 2-hop node and the node at $\mathbf{z}$ is a 1-hop node. For $k = 3$, we have $h_3(\mathbf{y},\mathbf{z})$ be the probability that the node at $\mathbf{y}$ is directly connected to the 2-hop node at $\mathbf{z}$ but not directly connected to the 1-hop node at $\mathbf{w}$. That is, the node at $\mathbf{y}$ is a "potential" 3-hop node as we do not specify whether the node at $\mathbf{y}$ is directly connected to the node at $\mathbf{x_0}$. Therefore, $h_3(\mathbf{y},\mathbf{z})$ has the meaning of being an upper bound for the probability that there exist a 3-hop node at $\mathbf{y}$ *and* a 2-hop node at $\mathbf{z}$ *and* the two nodes are directly connected. By recursion, $h_k(\mathbf{y},\mathbf{z})$ has the meaning of being an upper bound on the probability that there exist a k-hop node at $\mathbf{y}$ *and* a $(k-1)$-hop node at $\mathbf{z}$ *and* the two nodes are directly connected. Note that a node is a k-hop node if it is directly connected to at least one $(k-1)$-hop node and not directly connected to any of the i-hop nodes where $i < k-1$. Therefore using the union bound (with some arithmetic steps) and only considering the $(k-1)$-hop nodes and $(k-2)$-hop nodes, we obtain

$$\begin{aligned} E[N_k] &= \lim_{\Delta\to 0} \sum_{\mathbf{y}\in\mathbb{D}^d\setminus\{\mathbf{x_0}\}} \Pr\left\{I_{\mathbf{y}}^k = 1\right\} \\ &\le \lim_{\Delta\to 0} \sum_{\mathbf{y}\in\mathbb{D}^d\setminus\{\mathbf{x_0}\}} \sum_{\substack{\mathbf{z},\mathbf{w}\in\mathbb{D}^d\setminus\{\mathbf{y},\mathbf{x_0}\}\\ \mathbf{z}\neq\mathbf{w}}} \Big[\Pr\left\{J_{\mathbf{y}} = 1, H_{\mathbf{y},\mathbf{z}} = 1,\right. \\ &\qquad \left. H_{\mathbf{y},\mathbf{w}} = 0 \middle| I_{\mathbf{z}}^{k-1} = 1, I_{\mathbf{w}}^{k-2} = 1, H_{\mathbf{z},\mathbf{w}} = 1\right\} \\ &\quad \times \Pr\left\{I_{\mathbf{z}}^{k-1} = 1, I_{\mathbf{w}}^{k-2} = 1, H_{\mathbf{z},\mathbf{w}} = 1\right\}\Big] \\ &\qquad\qquad \text{[See Appendix B]} \quad (13) \\ &\le \lim_{\Delta\to 0} \sum_{\mathbf{y}\in\mathbb{D}^d\setminus\{\mathbf{x_0}\}} \sum_{\substack{\mathbf{z},\mathbf{w}\in\mathbb{D}^d\setminus\{\mathbf{y},\mathbf{x_0}\}\\ \mathbf{z}\neq\mathbf{w}}} [g(\mathbf{y}-\mathbf{z})[1-g(\mathbf{y}-\mathbf{w})] \\ &\quad \times [\lambda\delta\mathbf{y} + o(\delta\mathbf{y})] h_{k-1}(\mathbf{z},\mathbf{w})] \delta\mathbf{w}\delta\mathbf{z} \\ &= \int_{\mathbb{R}^d}\int_{\mathbb{R}^d} h_k(\mathbf{y},\mathbf{z}) d\mathbf{z}d\mathbf{y} \quad (14) \end{aligned}$$

and hence Eq. (6) is proved for generic k.

Next, we prove that $E[N_k]$ is finite by showing that the integral $\int_{\mathbb{R}^d}\int_{\mathbb{R}^d} h_k(\mathbf{y},\mathbf{z}) d\mathbf{z}d\mathbf{y}$ at the RHS of Eq. (6) is finite using mathematical induction. For $k = 1$, we have

$$E[N_1] = \int_{\mathbb{R}^d}\int_{\mathbb{R}^d} h_1(\mathbf{y},\mathbf{z}) d\mathbf{z}d\mathbf{y} = \int_{\mathbb{R}^d} \lambda g(\mathbf{y}-\mathbf{x_0}) d\mathbf{y} < \infty$$

due to the integral boundedness of the connection function $\bar{g}$. Suppose $\int_{\mathbb{R}^d}\int_{\mathbb{R}^d} h_{k-1}(\mathbf{y},\mathbf{z}) d\mathbf{y}d\mathbf{z} < \infty$, then

$$\begin{aligned} E[N_k] &\le \int_{\mathbb{R}^d}\int_{\mathbb{R}^d} h_k(\mathbf{y},\mathbf{z}) d\mathbf{z}d\mathbf{y} \qquad \text{[from Eq. (6)]} \\ &= \int_{\mathbb{R}^d}\int_{\mathbb{R}^d}\int_{\mathbb{R}^d} \lambda g(\mathbf{y}-\mathbf{z})[1-g(\mathbf{y}-\mathbf{w})] h_{k-1}(\mathbf{z},\mathbf{w}) d\mathbf{w}d\mathbf{z}d\mathbf{y} \\ &\le \int_{\mathbb{R}^d}\int_{\mathbb{R}^d}\int_{\mathbb{R}^d} \lambda g(\mathbf{y}-\mathbf{z}) h_{k-1}(\mathbf{z},\mathbf{w}) d\mathbf{w}d\mathbf{z}d\mathbf{y} \\ &\qquad \text{[since } 1-g(\mathbf{y}-\mathbf{w}) \le 1\text{]} \\ &= \int_{\mathbb{R}^d}\left[\int_{\mathbb{R}^d} \lambda g(\mathbf{y}-\mathbf{z}) d\mathbf{y}\right]\left[\int_{\mathbb{R}^d} h_{k-1}(\mathbf{z},\mathbf{w}) d\mathbf{w}\right] d\mathbf{z} \\ &= \left[\int_{\mathbb{R}^d} \lambda g(\mathbf{y}) d\mathbf{y}\right] \times \int_{\mathbb{R}^d}\int_{\mathbb{R}^d} h_{k-1}(\mathbf{z},\mathbf{w}) d\mathbf{w}d\mathbf{z} \\ &< \infty. \end{aligned}$$

■

On the basis of Lemma 1, the following theorem on a lower bound for λ_c can be obtained.

Theorem 2. *For $G(\mathcal{H}^d_{\lambda,\mathbf{x_0}}; \bar{g})$ with $d = 2, 3$ the critical density λ_c is lower bounded by*

$$\lambda_c \ge \sup_{m\in\mathbb{Z}^+} \left\{ \sqrt[m]{1/f_{\sup}(m)} \right\} \quad (15)$$

where

$$f_{\sup}(m) = \sup_{\mathbf{y_{m+1}},\mathbf{y_{m+2}}\in\mathbb{R}^d} \left\{ \int_{\mathbb{R}^d}\cdots\int_{\mathbb{R}^d} \left[\prod_{i=1}^{m} [g(\mathbf{y_i}-\mathbf{y_{i+1}}) [1-g(\mathbf{y_i}-\mathbf{y_{i+2}})]] \right] d\mathbf{y_1}\cdots d\mathbf{y_m} \right\}, \tag{16}$$

and $g(\mathbf{x}) = \bar{g}(\|\mathbf{x}\|)$ *for any* $\mathbf{x}\in\mathbb{R}^d$.

Proof: From Eq. (7), we have

$$\begin{aligned} &h_k(\mathbf{y_1},\mathbf{y_2}) \\ &= \int_{\mathbb{R}^d} \lambda g(\mathbf{y_1}-\mathbf{y_2})[1-g(\mathbf{y_1}-\mathbf{y_3})]h_{k-1}(\mathbf{y_2},\mathbf{y_3})d\mathbf{y_3} \\ &= \int_{\mathbb{R}^d}\cdots\int_{\mathbb{R}^d} \left[\prod_{i=1}^{m} [\lambda g(\mathbf{y_i}-\mathbf{y_{i+1}})[1-g(\mathbf{y_i}-\mathbf{y_{i+2}})]] \right] \\ &\quad \times h_{k-m}(\mathbf{y_{m+1}},\mathbf{y_{m+2}})d\mathbf{y_3}\cdots d\mathbf{y_{m+2}} \end{aligned} \tag{17}$$

for any integer $1\le m<k$. Using (16) and (17), it can be shown that

$$\begin{aligned} &\int_{\mathbb{R}^d}\int_{\mathbb{R}^d} h_k(\mathbf{y},\mathbf{z})d\mathbf{y}d\mathbf{z} \\ &\le \lambda^m f_{\sup}(m)\int_{\mathbb{R}^d}\int_{\mathbb{R}^d} h_{k-m}(\mathbf{y},\mathbf{z})d\mathbf{y}d\mathbf{z} \end{aligned} \tag{18}$$

for any integer $1\le m<k$. Applying Eq. (18) recursively into itself and using Eq. (6) we obtain

$$E[N_k] \le [\lambda^m f_{\sup}(m)]^{\lfloor \frac{k}{m} \rfloor} \int_{\mathbb{R}^d}\int_{\mathbb{R}^d} h_i(\mathbf{y},\mathbf{z})d\mathbf{y}d\mathbf{z} \tag{19}$$

where $i = k - \lfloor \frac{k}{m} \rfloor m$; $\lfloor a \rfloor$ is the largest integer smaller than or equal to a. Since $\int_{\mathbb{R}^d}\int_{\mathbb{R}^d} h_i(\mathbf{y},\mathbf{z})d\mathbf{y}d\mathbf{z} < \infty$ for any positive integer i (refer to the proof of Lemma 1), and $E[|\mathcal{W}|] = \sum_{k=1}^{\infty} E[N_k]$, Eq. (19) implies that $E[|\mathcal{W}|]$ is finite if $\lambda^m f_{\sup}(m) < 1$. Given the fact that $E[|\mathcal{W}|]$ is finite implies $\theta(\lambda) = 0$ [17, Theorem 6.1], we have $\lambda_c \ge \sqrt[m]{1/f_{\sup}(m)}$ for all positive integer m. The result follows. ∎

Alternatively, Theorem 2 can be rewritten as follows.

Theorem 3. *For* $G(\mathcal{H}^d_{\lambda,\mathbf{x_0}};\bar{g})$ *with* $d=2,3$ *the critical density* λ_c *is lower bounded by*

$$\lambda_c \ge \sup_{m\in\mathbb{Z}^+} \left\{ \sqrt[m]{1/f_{\sup}(m)} \right\} = \lim_{m\to\infty} \left\{ \sqrt[m]{1/f_{\sup}(m)} \right\} \tag{20}$$

where $f_{\sup}(m)$ *is given in Eq.* (16)*.*

The proof of Theorem 3 relies on the following lemma from [32].

Lemma 2 (Lemma 2.1 in [32])**.** *Let* $(a_n)_{n\in\mathbb{N}}$ *be a sequence of elements of* $\mathbb{R}^+\cup\{\infty\}$ *such that*

$$a_{n+m} \le a_n a_m \qquad \text{for all } n,m\in\mathbb{N}.$$

If $a_1<\infty$*, then* $a_n<\infty$ *for all* $n\in\mathbb{N}$*, the sequence* $\left(a_n^{1/n}\right)_{n\in\mathbb{N}}$ *is convergent and*

$$\lim_{n\to\infty} a_n^{1/n} \le a_m^{1/m} \quad \text{for each } m\in\mathbb{N}.$$

On the basis of Lemma 2, we can prove Theorem 3 as follows.

Proof of Theorem 3: From Eq. (16), we have for all $n,m\in\mathbb{Z}^+$,

$$\begin{aligned} &f_{\sup}(m+n) \\ &= \sup_{\mathbf{y_{m+n+1}},\mathbf{y_{m+n+2}}\in\mathbb{R}^d} \left\{ \int_{\mathbb{R}^d}\cdots\int_{\mathbb{R}^d} \left[\prod_{i=1}^{m+n} [g(\mathbf{y_i}-\mathbf{y_{i+1}}) [1-g(\mathbf{y_i}-\mathbf{y_{i+2}})]] \right] d\mathbf{y_1}\cdots d\mathbf{y_{m+n}} \right\} \\ &= \sup_{\mathbf{y_{m+n+1}},\mathbf{y_{m+n+2}}\in\mathbb{R}^d} \left\{ \int_{\mathbb{R}^d}\cdots\int_{\mathbb{R}^d} \left[\int_{\mathbb{R}^d}\cdots\int_{\mathbb{R}^d} \left[\prod_{i=1}^{m} [g(\mathbf{y_i}-\mathbf{y_{i+1}})[1-g(\mathbf{y_i}-\mathbf{y_{i+2}})]] \right] d\mathbf{y_1}\cdots d\mathbf{y_m} \right] \right. \\ &\qquad \left. \left[\prod_{i=m+1}^{m+n} [g(\mathbf{y_i}-\mathbf{y_{i+1}})[1-g(\mathbf{y_i}-\mathbf{y_{i+2}})]] \right] d\mathbf{y_{m+1}}\cdots d\mathbf{y_{m+n}} \right\} \\ &\le \sup_{\mathbf{y_{m+1}},\mathbf{y_{m+2}}\in\mathbb{R}^d} \left\{ \int_{\mathbb{R}^d}\cdots\int_{\mathbb{R}^d} \left[\prod_{i=1}^{m} [g(\mathbf{y_i}-\mathbf{y_{i+1}}) [1-g(\mathbf{y_i}-\mathbf{y_{i+2}})]] \right] d\mathbf{y_1}\cdots d\mathbf{y_m} \right\} \\ &\quad \times \sup_{\mathbf{y_{m+n+1}},\mathbf{y_{m+n+2}}\in\mathbb{R}^d} \left\{ \int_{\mathbb{R}^d}\cdots\int_{\mathbb{R}^d} \left[\prod_{i=m+1}^{m+n} [g(\mathbf{y_i}-\mathbf{y_{i+1}}) [1-g(\mathbf{y_i}-\mathbf{y_{i+2}})]] \right] d\mathbf{y_{m+1}}\cdots d\mathbf{y_{m+n}} \right\} \end{aligned} \tag{21}$$

$$= f_{\sup}(m) f_{\sup}(n) \tag{22}$$

where Eq. (21) follows from the monotonicity of integral. Furthermore,

$$\begin{aligned} f_{\sup}(1) &= \sup_{\mathbf{y_2},\mathbf{y_3}\in\mathbb{R}^d} \left\{ \int_{\mathbb{R}^d} [g(\mathbf{y_1}-\mathbf{y_2})[1-g(\mathbf{y_1}-\mathbf{y_3})]]\, d\mathbf{y_1} \right\} \\ &= \sup_{\mathbf{y_3}\in\mathbb{R}^d} \left\{ \int_{\mathbb{R}^d} [g(\mathbf{y_1})[1-g(\mathbf{y_1}-\mathbf{y_3})]]\, d\mathbf{y_1} \right\} \\ &\le \int_{\mathbb{R}^d} g(\mathbf{y})d\mathbf{y} \qquad < \infty. \end{aligned} \tag{23}$$

Eq. (22), (23) and Lemma 2 together show that the sequence $\left(\sqrt[m]{f_{\sup}(m)}\right)_{m\in\mathbb{Z}^+}$ is convergent and

$$\begin{aligned} &\lim_{m\to\infty} \sqrt[m]{f_{\sup}(m)} \le \sqrt[n]{f_{\sup}(n)} \qquad \text{for each } n\in\mathbb{Z}^+ \\ \Leftrightarrow\ &\lim_{m\to\infty} \sqrt[m]{f_{\sup}(m)} = \inf_{n\in\mathbb{Z}^+} \left\{ \sqrt[n]{f_{\sup}(n)} \right\}. \end{aligned} \tag{24}$$

With Eq. (24) and Theorem 2, the result follows. ∎

Remark 1. Although we consider $G(\mathcal{H}^d_{\lambda,\mathbf{x_0}};\bar{g})$ with $d=2,3$ in Lemma 1, Theorem 2 and 3, it can be seen from their proofs that they are applicable to arbitrary integer d. Note that this is not the case for Theorem 4 and 5 in Section V.

B. Discussion

In this subsection, we compare our lower bound with the existing results in the literature obtained under the unit disk

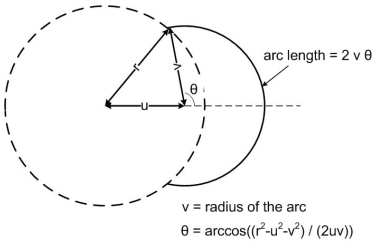

Fig. 1. Arc length calculation related to $f_{\sup}(2)$ in $\mathbb{R}^2$ under the unit disk model.

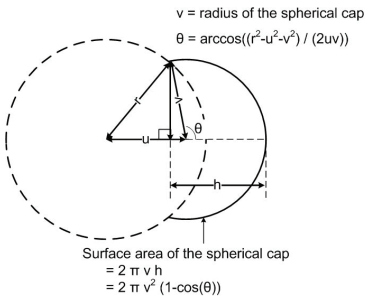

Fig. 2. (2D view) Surface area calculation of a spherical cap related to $f_{\sup}(2)$ in $\mathbb{R}^3$ under the unit disk model.

model and the log-normal model which are two special cases of the random connection model.

To obtain the lower bound under the unit disk model, we apply Eq. (2) into (16) and yield

$$f_{\sup}(1) = \sup_{\mathbf{y_2},\mathbf{y_3}\in\mathbb{R}^d} \left\{ \int_{\mathbb{R}^d} g(\mathbf{y_1}-\mathbf{y_2})[1-g(\mathbf{y_1}-\mathbf{y_3})]d\mathbf{y_1} \right\} = \int_{\|\mathbf{y_1}\|\le r} d\mathbf{y_1} = V_d r^d, \tag{25}$$

where $V_d = \frac{\pi^{d/2}}{\Gamma(\frac{d}{2}+1)}$ is the volume of $(d-1)$-sphere with unit radius; $\Gamma(.)$ is the gamma function. Similarly,

$$f_{\sup}(2) = \sup_{\mathbf{y_3},\mathbf{y_4}\in\mathbb{R}^d} \left\{ \int_{\mathbb{R}^d}\int_{\mathbb{R}^d} g(\mathbf{y_1}-\mathbf{y_2})[1-g(\mathbf{y_1}-\mathbf{y_3})] \times g(\mathbf{y_2}-\mathbf{y_3})[1-g(\mathbf{y_2}-\mathbf{y_4})]d\mathbf{y_1}d\mathbf{y_2} \right\} = \int_{\|\mathbf{y_2}\|\le r}\int_{\|\mathbf{y_1}-\mathbf{y_2}\|\le r,\|\mathbf{y_1}\|>r} d\mathbf{y_1}d\mathbf{y_2}. \tag{26}$$

For $d = 2$, Eq. (26) can be simplified to

$$f_{\sup}(2) = \int_0^r \left[\int_{r-u}^r 2v \arccos\left(\frac{r^2-u^2-v^2}{2uv}\right)dv \right] 2\pi u du \tag{27}$$

which is obtained using elementary geometric calculations for finding an arc length, as illustrated in Fig. 1; for $d = 3$, Eq. (26) can be simplified to

$$f_{\sup}(2) = \int_0^r \left[\int_{r-u}^r 2\pi v^2 \left(1-\frac{r^2-u^2-v^2}{2uv}\right)dv \right] 4\pi u^2 du \tag{28}$$

which follows from elementary geometric calculations for finding the curved surface area of a spherical cap [33], as illustrated in Fig. 2.

Using a similar approach as that in Eq. (27) and (28) we can extend and generalize the calculation of $f_{\sup}(m)$ under the unit disk model for $m \ge 3$, i.e. considering $\|\mathbf{y_i}-\mathbf{y_{i+1}}\| \le r$ and $\|\mathbf{y_i}-\mathbf{y_{i+2}}\| > r$ (for all $1 \le i \le m-2$) for the integrations in Eq. (16). Then we obtain the lower bound for λ_c using Theorem 2. The result is shown with other existing results in the literature in Fig. 3 and 4.

Fig. 3 shows that our lower bound in $\mathbb{R}^2$ is as tight as the lower bound obtained by Meester and Roy [17]. The lower bounds reported by Kong and Yeh [19], and Gu and Hong [28] are tighter than our lower bound, however their results are valid for the unit disk model only. In this paper we

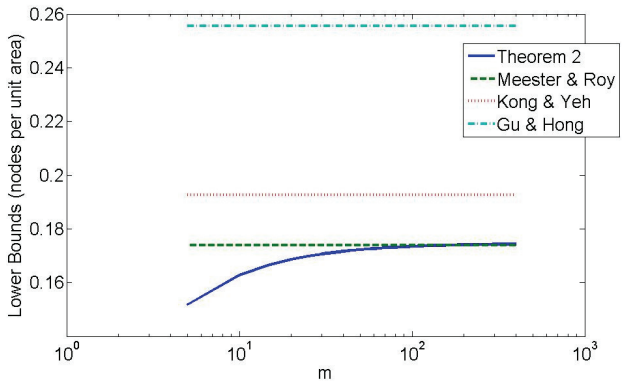

Fig. 3. Lower bounds for λ_c in $\mathbb{R}^2$ under the unit disk model with $r = 2$.

consider the random connection model which is applicable to broader class of connection model, including the unit disk model. On the other hand, Fig. 4 also shows that our lower bound in $\mathbb{R}^3$ is not as tight as the bound obtained by Kong and Yeh [19] (though it is within 6%). The tightness of our lower bound largely depends on how the distribution of the k-hop nodes is obtained. When we obtain the distribution of the k-hop nodes through the technique in Lemma 1, we only consider the impact of the previous two hops, i.e. $(k-1)$-hop nodes and $(k-2)$-hop nodes, on the distribution of the k-hop nodes. The impact of nodes three or more hops away are not taken into account. The tightness of our lower bound is therefore sacrificed for simplicity. A tighter lower bound can be achieved if we take into account the impact of nodes three or more hops away. However it will involve more complex analysis.

To obtain the lower bound under the log-normal model, we first apply Eq. (3) into (16). Then the lower bound under the log-normal model can be calculated by using a similar approach to that used in obtaining the lower bound under the unit disk model, which involves converting Eq. (16) from Cartesian coordinate system to Polar coordinate system in $\mathbb{R}^2$ or Spherical coordinate system in $\mathbb{R}^3$. Due to its complexity, the end form of the equation is omitted here. Instead, the results are plotted in Fig. 5 and 6 but with no comparison to bounds from another method, since we know of none.[1]

[1]In order to have a fairer comparison between lower bounds under the log-normal model with different shadowing variance, the results in Fig. 5 and 6 have been normalized so that the average node degree is preserved while changing the shadowing variance. Similarly for Fig. 10 and 11 in the next section.

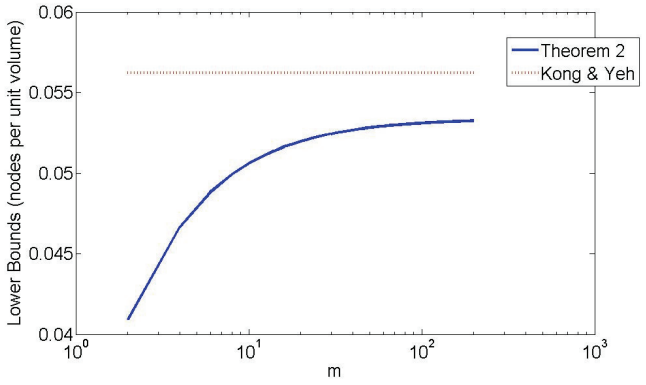

Fig. 4. Lower bounds for λ_c in $\mathbb{R}^3$ under the unit disk model with $r = 2$.

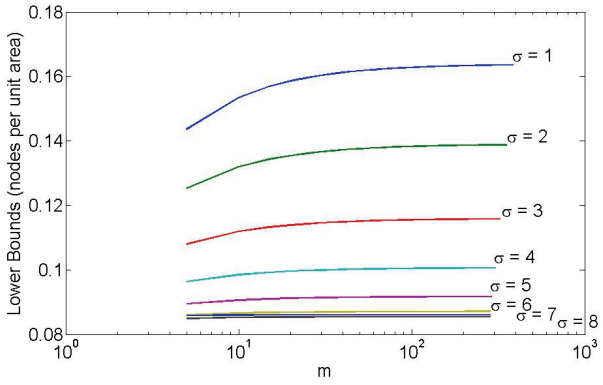

Fig. 5. Our lower bounds for λ_c in $\mathbb{R}^2$ under the log-normal model with different shadowing variances. (No other lower bounds are found in the literature)

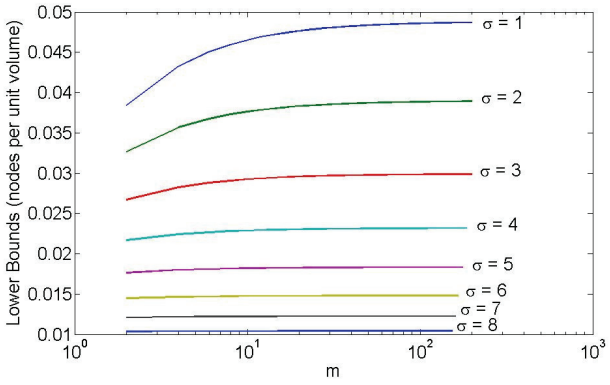

Fig. 6. Our lower bounds for λ_c in $\mathbb{R}^3$ under the log-normal model with different shadowing variances. (No other lower bounds are found in the literature)

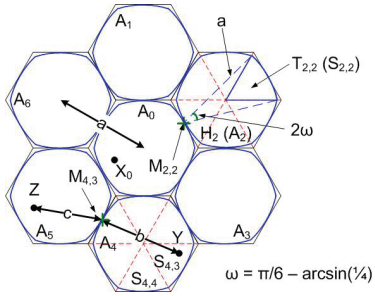

Fig. 7. The hexagons and the flower-shape cell in each hexagon: The partition of each hexagon into six non-overlapping equilateral triangles and construction of an intersectional area inside each triangle is illustrated in hexagon H_2. An example of how the distance b is defined for a node is shown in flower-shape cell A_4.

V. Upper Bound for λ_c

A. Analysis

First, we consider the problem in $\mathbb{R}^2$ as follows. Let us partition the $\mathbb{R}^2$ plane into non-overlapping hexagons, where the distance between the centers of two neighboring hexagons is $a > 0$. We further partition each hexagon into six non-overlapping equilateral triangles. As shown in Fig. 7, the hexagon labeled H_2 is partitioned into six triangles. Consider a hexagon (e.g. H_2 in Fig. 7) and an equilateral triangle (e.g. $T_{2,2}$) in the hexagon, there is exactly one hexagon side which is located directly opposite to the triangle. Centered at the middle point of that hexagon side (i.e. $M_{2,2}$), we draw a circle with radius a and obtain its intersectional area with the triangle (i.e. $S_{2,2}$). Repeat the action for the other five equilateral triangles in the hexagon. Merging the six intersectional areas we obtain a flower-shape cell within the hexagon (i.e. A_2).

Next, we want to obtain a lower bound for the probability that any two nodes inside two neighboring flower-shape cells are directly connected. Consider two neighboring flower-shape cells, e.g. A_4 and A_5 in Fig. 7, and two nodes Y and Z (one in each cell). Among the six intersectional areas in A_4, consider Y is located in the intersectional area which is furthest to A_5, i.e. $S_{4,3}$ in A_4. Denote by b the Euclidean distance between the node and the middle point (i.e. $M_{4,3}$) of the hexagon side shared by A_4 and A_5. Then we have $b \in [\frac{a}{2}, a]$. Consider Z is located anywhere within A_5 and denote by c the Euclidean distance between Z and the middle point $M_{4,3}$. Due to triangular inequality, the distance between Y and Z is less than or equal to $b+c$. Since $c \leq a$, it can then be easily shown that the distance between Y and a node in A_5 is at most $b+a$. Let $f_a(b)$ be the pdf (probability density function) of the above defined distance b. By elementary geometric calculations,

$$f_a(b) = \frac{12b}{|A(a)|}\left[\frac{\pi}{6} - \arcsin(\frac{a}{4b})\right] \tag{29}$$

where $|A(a)|$ is the area of a flower-shape cell and is given by

$$|A(a)| = 6a^2\left[\omega - \frac{1}{2}\sin(\omega)\right] \tag{30}$$

with $\omega = \frac{\pi}{6} - \arcsin(\frac{1}{4})$ (see also Fig. 7). Due to the non-increasing monotonicity property of $\bar{g}$, the probability that Y is directly connected to any node in A_0 is lower bounded by $\bar{g}(b+a)$. Therefore, the probability that any two nodes inside two neighboring flower-shape cells are directly connected, denoted by $\bar{p}(a)$, satisfies the following condition:

$$\bar{p}(a) \geq \int_{a/2}^{a} \bar{g}(b+a) f_a(b) db \triangleq \hat{p}(a). \tag{31}$$

Now, starting with the flower-shape cell A_0 with a node X_0 located anywhere within it, we examine the connections between X_0 and the nodes in the six neighboring flower-shape cells, $A_1, A_2, \cdots, A_6$ (see Fig. 7). We say A_i, $1 \leq i \leq 6$, is

"*occupied*" if and only if there exists at least one node in A_i, *and* X_0 is directly connected to at least one of the nodes in A_i. The probability that A_i (with size $|A(a)|$) is "occupied", denoted by p, is then

$$\begin{aligned} p >& \sum_{m=1}^{\infty} \left[\frac{[\lambda|A(a)|]^m \exp(-\lambda|A(a)|)}{m!} \times [1-[1-\hat{p}(a)]^m] \right] \\ =& \left[1-e^{-\lambda|A(a)|}\right] - e^{-\lambda|A(a)|\hat{p}(a)} \left[1-e^{-\lambda|A(a)|(1-\hat{p}(a))}\right] \\ =& 1-e^{-\lambda|A(a)|\hat{p}(a)}. \end{aligned} \tag{32}$$

Note that the events that neighboring flower-shape cells are "occupied" are independent. Next, for each A_i marked as "occupied" we focus on a node X_i in A_i which is directly connected to X_0 and examine the direct connections from X_i to other nodes in the neighboring flower-shape cells that have not been considered before. The process continues in a similar way until every flower-shape cell is marked to be either "occupied" or "empty".

Following from the above marking process, it can be seen that $\Pr\{|\mathcal{W}|=\infty\} > 0$ *if* the probability that there are infinite number of flower-shape cells which are marked as "occupied" is positive. We say that the flower-shape cells percolate if there are infinite number of flower-shape cells marked as "occupied". Imagine we replace each flower-shape cell by a vertex and draw an edge between two neighboring vertices. Then the vertices form an equilateral triangular lattice. If the vertices inherit the status of respective flower-shape cells, i.e. a vertex is marked as "occupied" if and only if the corresponding flower-shape cell is marked as "occupied", then the site percolation on the accompanying equilateral triangular lattice implies the percolation of the flower-shape cells, and vice versa. Hence, the flower-shape cells percolates if $p > 0.5$ [23, p. 132]. That is, $\Pr\{|\mathcal{W}|=\infty\} > 0$ if

$$1-e^{-\lambda|A(a)|\hat{p}(a)} > 0.5 \Leftrightarrow \lambda > \frac{\log_e(2)}{|A(a)|\hat{p}(a)}. \tag{33}$$

Indeed, $\Pr\{|\mathcal{W}|=\infty\} > 0$ if Eq. (33) holds *for any* value of a. The above analysis can be summarized into the following theorem.

Theorem 4. *For $G(\mathcal{H}^2_{\lambda,\mathbf{x_0}}; \bar{g})$ the critical density λ_c is upper bounded by*

$$\lambda_c \leq \inf_{a\in\mathbb{R}^+} \left\{ \frac{\log_e(2)}{12\int_{a/2}^{a} b\bar{g}(b+a)\left[\frac{\pi}{6}-\arcsin(\frac{a}{4b})\right]db} \right\}. \tag{34}$$

Remark 2. In Theorem 4, we obtain an upper bound for λ_c using the pdf of b which is given in Eq. (29). Note that Eq. (29) is obtained by considering a node located in just one of the six intersectional areas in a flower-shape cell. Particularly, the chosen intersectional area is the one which will maximize the distance b. An improved upper bound can be obtained by considering the situation that the node can be located in any intersectional area within the flowers-shape cell. However, due to the difficulty in computing the pdf of b, no close form can be obtained for the upper bound. Therefore, we continue to use the existing approach to obtain an upper bound in $\mathbb{R}^2$ and later in $\mathbb{R}^3$. In Fig. 10, the improved upper bound is plotted numerically.

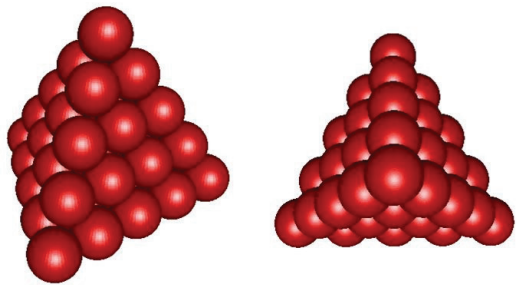

Fig. 8. Face-centered cubic (fcc) packing of equal spheres.

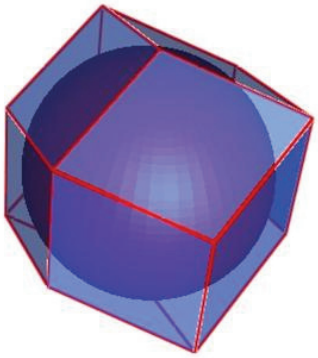

Fig. 9. Rhombic dodecahedron as the shape of the Voronoi cells.

To extend the above analysis for $\mathbb{R}^2$ to $\mathbb{R}^3$, we first partition the $\mathbb{R}^3$ space into non-overlapping rhombic dodecahedra. The logic behind the transformation from hexagons in $\mathbb{R}^2$ to rhombic dodecahedra in $\mathbb{R}^3$ is related to the close-packing of equal-radius $(d-1)$-spheres in $\mathbb{R}^d$. In $\mathbb{R}^2$, the hexagon is the shape of the Voronoi cells constructed from the equilateral triangular lattice [34], the densest arrangement of equal-radius disks in $\mathbb{R}^2$ [35, p. 6]; in $\mathbb{R}^3$, the rhombic dodecahedron is the shape of the Voronoi cells constructed from the fcc (face-centered cubic) lattice [35, p. 34], one of the densest possible arrangements of equal-radius spheres in $\mathbb{R}^3$ [34]. Refer to Fig. 8 and 9 for the visualization of fcc packing of equal-radius spheres and rhombic dodecahedron, the shape of the associated Voronoi cells.

Using the similar approach in $\mathbb{R}^2$, we then construct a 3D flower-shape cell within each rhombic dodecahedron so that the maximum Euclidean distance between any pair of nodes within two neighboring flower-shape cells is $2a$, where a is the distance between the centers of two neighboring rhombic dodecahedra. Based on the constructed flower-shape cells, we can rewrite Eq. (29) into

$$\begin{aligned} & f_a(b) \\ =& \frac{48b^2}{|V(a)|}\int_{\theta_{\min}}^{\frac{\pi}{2}} \sin(\theta)\left[\frac{\pi}{4}-\arcsin(\frac{a/2+\sqrt{2}b\cos(\theta)}{\sqrt{2}b\sin(\theta)})\right]d\theta \end{aligned} \tag{35}$$

where $\theta_{\min} = \frac{\pi}{2} - \arcsin(\frac{1}{\sqrt{3}}) + \arcsin(\frac{a}{2\sqrt{3}b})$ and $|V(a)|$ is the volume of a 3D flower-shape cell. Substituting Eq. (35) into Eq. (31), and bearing in mind that the site percolation on the fcc lattice (where the critical probability is approximately

0.199 [36]) implies the site percolation of the flower-shape cells, we obtain the follow theorem.

Theorem 5. *For $G(\mathcal{H}^3_{\lambda,\mathbf{x_0}};\bar{g})$ the critical density λ_c is upper bounded by*

$$\lambda_c \leq \inf_{a\in\mathbb{R}^+}\left\{-\frac{\log_e(0.801)}{\int_{\frac{a}{2}}^{a}\bar{g}(b+a)\bar{f}_a(b)db}\right\} \tag{36}$$

where

$$\bar{f}_a(b) = 48b^2\int_{\theta_{\min}}^{\pi/2}\sin(\theta)\left[\frac{\pi}{4}-\arcsin(\frac{a/2+\sqrt{2}b\cos(\theta)}{\sqrt{2}b\sin(\theta)})\right]d\theta,$$

and $\theta_{\min} = \frac{\pi}{2}-\arcsin(\frac{1}{\sqrt{3}})+\arcsin(\frac{a}{2\sqrt{3}b})$.

B. Discussion

To illustrate the tightness of our upper bound, we compare our result with the existing upper bound in the literature obtained under the unit disk model [17], [27], [28] and the log-normal model [29].

To obtain the upper bound in $\mathbb{R}^2$ under the unit disk model, first let $\lambda^{(r)}_{upper}$ be the upper bound for λ_c under the unit disk model with transmission range r. Applying Eq. (2) into (34), it can be shown that the infimum is achieved at $a=\frac{1}{2}r$. That is,

$$\lambda^{(r)}_{upper} = \frac{\log_e(2)}{|A(r/2)|} = \frac{\log_e(2)}{\frac{3}{2}r^2\left[\omega-\frac{1}{2}\sin(\omega)\right]} \tag{37}$$

with $\omega=\frac{\pi}{6}-\arcsin(\frac{1}{4})$. Then Eq. (34) reduces to the upper bound obtained in [17], [28]. As a specific example with $r=2$, we have $\lambda^{(2)}_{upper}\approx 0.843$ and it is shown in Fig. 10 (as the log-normal model with $\sigma=0$). On the other hand, it means that our upper bound is not as tight as the upper bound obtained by Philips et al. [27] (0.8376 for $r=2$). In our approach to obtain the upper bound, the constructed flower-shape cells must lie inside the corresponding hexagons. Then we consider the nodes that fall inside each flower-shape cell. In contrast, Philips et al. [27] allow some portion of each flower-shape cell to exceed the boundary of the corresponding hexagon. Then they consider those nodes that fall inside both flower-shape cell *and* the corresponding hexagon. The ratio of flower-shape cell size to hexagon size is adjusted to obtain the tightest upper bound. The approach used in [27] can be adapted into our analysis to achieve a tighter upper bound. However, it will involve more complex analysis.

The upper bound in $\mathbb{R}^2$ under the log-normal model can be calculated by substituting Eq. (3) into (34). The end form of the equation is omitted due to its complexity. To compare our result with other upper bounds in the literature [29], first let

$$\lambda_{upper}(\bar{g}) = \inf_{a\in\mathbb{R}^+}\left\{\frac{\log_e(2)}{12\int_{a/2}^{a}b\bar{g}(b+a)\left[\frac{\pi}{6}-\arcsin(\frac{a}{4b})\right]db}\right\} \tag{38}$$

be the upper bound for λ_c given by Eq. (34). From Eq. (38),

$$\lambda_{upper}(\bar{g}) \leq \inf_{a\in\mathbb{R}^+}\left\{\frac{\log_e(2)}{|A(a)|\bar{g}(2a)}\right\}$$

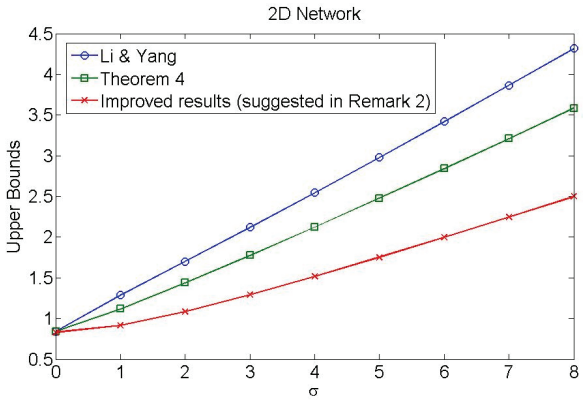

Fig. 10. Upper bounds for λ_c in $\mathbb{R}^2$ under the log-normal model with different shadowing variances and $r=2$, $\alpha=2$. Note that the log-normal model reduces to the unit disk model when $\sigma=0$.

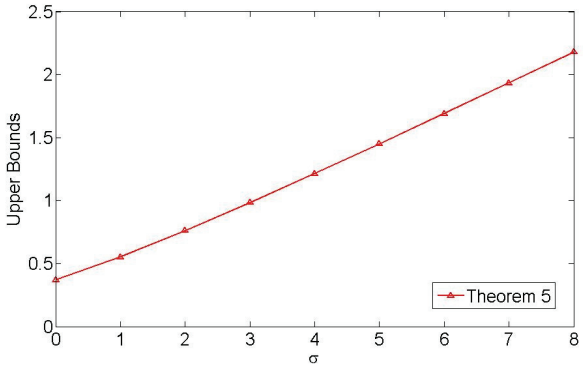

Fig. 11. Upper bounds for λ_c in $\mathbb{R}^3$ under the log-normal model with different shadowing variances and $r=2$, $\alpha=2$. Note that the log-normal model reduces to the unit disk model when $\sigma=0$. (No other upper bounds under the log-normal model are found in the literature)

$$= \inf_{a\in\mathbb{R}^+}\left\{\frac{\log_e(2)}{|A(a/2)|\bar{g}(a)}\right\} = \inf_{a\in\mathbb{R}^+}\left\{\frac{\lambda^{(1)}_{upper}}{a^2\bar{g}(a)}\right\} \tag{39}$$

where $\lambda^{(1)}_{upper}$ is given by Eq. (37) with $r=1$. Note that the RHS of Eq. (39) was reported by Li and Yang [29] but only for the log-normal model. The derivation of Eq. (39) shows that Theorem 4 provides a tighter upper bound than that in [29] (see Fig. 10 for an illustration).

To the best of our knowledge, no upper bound has been obtained in $\mathbb{R}^3$ under either the unit disk model or the log-normal model. An illustration of the upper bound in Theorem 5 is shown in Fig. 11.

VI. Conclusions and Future Work

In this paper we investigated the analytical bounds for the critical density in wireless multi-hop networks where nodes are Poissonly distributed in $\mathbb{R}^d$ ($d=2,3$). The establishment of direct connection between two nodes follows a random connection model satisfying some intuitively reasonable conditions, viz. rotational and translation invariance, non-increasing monotonicity and integral boundedness. We obtained a lower bound for the critical density using a Galton-Watson branching process and an upper bound by relating the

problem to that of site percolation on a lattice. From the above generic results, we then obtained the bounds under the unit disk model and the log-normal model, which are special cases of the random connection model, and compared them with the existing results in the literature. The outcome showed that our method generates bounds that are either close to or tighter than the existing results in the literature, apart from being more generic. In future work, we plan to extend the current work in two directions. First, at the cost of substantially more calculations, our bounds can be improved as both our lower and upper bounds are not the tightest bounds under the unit disk model. Second, techniques that can analytically and accurately estimate the value of the critical density will be investigated.

APPENDIX A
DERIVATION OF EQ. (11)

In this section, we follow the definitions and notations used in Lemma 1. Note that if a node Y is a 2-hop node, then it is not directly connected to the node at $\mathbf{x_0}$ but directly connected to at least one 1-hop nodes. Recall that N_1 is a random variable denoting the number of 1-hop nodes; hence for any positive integer n_1 we have

$$\begin{aligned}
&\Pr\left\{ I^2_{\mathbf{y}}=1, \bigcap_{i=1}^{n_1} I^1_{\mathbf{z_i}}=1 \middle| N_1=n_1 \right\} \\
=&\Pr\left\{ J_{\mathbf{y}}=1, H_{\mathbf{y},\mathbf{x_0}}=0, \bigcup_{i=1}^{n_1} H_{\mathbf{y},\mathbf{z_i}}=1, \bigcap_{i=1}^{n_1} I^1_{\mathbf{z_i}}=1 \middle| N_1=n_1 \right\} \\
\le&\sum_{j=1}^{n_1} \Pr\left\{ J_{\mathbf{y}}=1, H_{\mathbf{y},\mathbf{x_0}}=0, H_{\mathbf{y},\mathbf{z_j}}=1, \bigcap_{i=1}^{n_1} I^1_{\mathbf{z_i}}=1 \middle| N_1=n_1 \right\} \\
&\qquad \text{[union bound].} \qquad (40)
\end{aligned}$$

The conditional probability $\Pr\left\{ I^2_{\mathbf{y}}=1 \middle| N_1=n_1 \right\}$ is then obtained as follows.

$$\begin{aligned}
&\Pr\left\{ I^2_{\mathbf{y}}=1 \middle| N_1=n_1 \right\} \\
=&\frac{1}{n_1!} \sum_{\substack{\mathbf{z_1},\cdots,\mathbf{z_{n_1}}\in\mathbb{D}^d\setminus\{\mathbf{y},\mathbf{x_0}\} \\ \mathbf{z_m}\neq\mathbf{z_n} \text{ for } m\neq n}} \Pr\left\{ I^2_{\mathbf{y}}=1, \bigcap_{i=1}^{n_1} I^1_{\mathbf{z_i}}=1 \middle| N_1=n_1 \right\} \\
\le&\frac{1}{n_1!} \sum_{\substack{\mathbf{z_1},\cdots,\mathbf{z_{n_1}}\in\mathbb{D}^d\setminus\{\mathbf{y},\mathbf{x_0}\} \\ \mathbf{z_m}\neq\mathbf{z_n} \text{ for } m\neq n}} \sum_{j=1}^{n_1} \Pr\left\{ J_{\mathbf{y}}=1, H_{\mathbf{y},\mathbf{x_0}}=0, \right. \\
&\qquad \left. H_{\mathbf{y},\mathbf{z_j}}=1, \bigcap_{i=1}^{n_1} I^1_{\mathbf{z_i}}=1 \middle| N_1=n_1 \right\} \qquad \text{[from Eq. (40)]} \\
=&\frac{1}{n_1!} \sum_{j=1}^{n_1} \sum_{\mathbf{z_j}\in\mathbb{D}^d\setminus\{\mathbf{y},\mathbf{x_0}\}} \left[\sum_{\substack{\mathbf{z_1},\cdots,\mathbf{z_{j-1}},\mathbf{z_{j+1}},\cdots,\mathbf{z_{n_1}}\in\mathbb{D}^d\setminus\{\mathbf{y},\mathbf{x_0},\mathbf{z_j}\} \\ \mathbf{z_m}\neq\mathbf{z_n} \text{ for } m\neq n}} \Pr\left\{ J_{\mathbf{y}}=1, \right. \right. \\
&\qquad \left. \left. H_{\mathbf{y},\mathbf{x_0}}=0, H_{\mathbf{y},\mathbf{z_j}}=1, \bigcap_{i=1}^{n_1} I^1_{\mathbf{z_i}}=1 \middle| N_1=n_1 \right\} \right] \\
&\text{[move the summation on } j \text{ and } \mathbf{z_j} \text{ to the outermost]} \\
=&\frac{1}{n_1!} \sum_{j=1}^{n_1} \sum_{\mathbf{z_j}\in\mathbb{D}^d\setminus\{\mathbf{y},\mathbf{x_0}\}} \left[(n_1-1)! \Pr\left\{ J_{\mathbf{y}}=1, H_{\mathbf{y},\mathbf{x_0}}=0, \right. \right. \\
&\qquad \left. \left. H_{\mathbf{y},\mathbf{z_j}}=1, I^1_{\mathbf{z_j}}=1 \middle| N_1=n_1 \right\} \right] \\
&\text{[resolve the summations inside the square brackets]} \\
=&\sum_{\mathbf{z}\in\mathbb{D}^d\setminus\{\mathbf{y},\mathbf{x_0}\}} \left[\Pr\{ J_{\mathbf{y}}=1, H_{\mathbf{y},\mathbf{x_0}}=0, H_{\mathbf{y},\mathbf{z}}=1 | \right. \\
&\qquad \left. I^1_{\mathbf{z}}=1, N_1=n_1 \right\} \Pr\left\{ I^1_{\mathbf{z}}=1 \middle| N_1=n_1 \right\} \Big]. \qquad (41)
\end{aligned}$$

Since

$$\Pr\left\{ I^1_{\mathbf{z}}=1 \middle| N_1=n_1 \right\} = \frac{\Pr\left\{ I^1_{\mathbf{z}}=1, N_1=n_1 \right\}}{\Pr\{N_1=n_1\}} \qquad (42)$$

and

$$\sum_{n_1=1}^{\infty} \Pr\left\{ I^1_{\mathbf{z}}=1, N_1=n_1 \right\} = \Pr\left\{ I^1_{\mathbf{z}}=1 \right\}, \qquad (43)$$

using Eq. (41), (42) and (43) we obtain

$$\begin{aligned}
&\Pr\left\{ I^2_{\mathbf{y}}=1 \right\} \\
=&\sum_{n_1=1}^{\infty} \left[\Pr\left\{ I^2_{\mathbf{y}}=1 \middle| N_1=n_1 \right\} \Pr\{N_1=n_1\} \right] \\
\le&\sum_{\mathbf{z}\in\mathbb{D}^d\setminus\{\mathbf{y},\mathbf{x_0}\}} \left[\Pr\left\{ J_{\mathbf{y}}=1, H_{\mathbf{y},\mathbf{x_0}}=0, H_{\mathbf{y},\mathbf{z}}=1 \middle| I^1_{\mathbf{z}}=1 \right\} \right. \\
&\qquad \left. \times \Pr\left\{ I^1_{\mathbf{z}}=1 \right\} \right]. \qquad (44)
\end{aligned}$$

Hence we obtain Eq. (11).

APPENDIX B
DERIVATION OF EQ. (13)

In this section, we follow the definitions and notations used in Lemma 1. The upper bound for the probability that a k-hop node exists within $B_{\mathbf{y}}$ conditioned on the event that $\{N_{k-2}=n_{k-2}\}$ is obtained as follows.

$$\begin{aligned}
&\Pr\left\{ I^k_{\mathbf{y}}=1 \middle| N_{k-2}=n_{k-2} \right\} \\
=&\frac{1}{n_{k-2}!} \sum_{\substack{\mathbf{w_1},\cdots,\mathbf{w_{n_{k-2}}}\in\mathbb{D}^d\setminus\{\mathbf{y},\mathbf{x_0}\} \\ \mathbf{w_m}\neq\mathbf{w_n} \text{ for } m\neq n}} \Pr\left\{ I^k_{\mathbf{y}}=1, \bigcap_{i=1}^{n_{k-2}} I^{k-2}_{\mathbf{w_i}}=1 \middle| \right. \\
&\qquad \left. N_{k-2}=n_{k-2} \right\}. \qquad (45)
\end{aligned}$$

By generalizing the derivation of Eq. (44), it can be shown that,

$$\begin{aligned}
&\Pr\left\{ I^k_{\mathbf{y}}=1, \bigcap_{i=1}^{n_{k-2}} I^{k-2}_{\mathbf{w_i}}=1 \middle| N_{k-2}=n_{k-2} \right\} \\
\le&\sum_{\mathbf{z}\in\mathbb{D}^d\setminus\{\mathbf{y},\mathbf{x_0}\}} \Pr\left\{ J_{\mathbf{y}}=1, \bigcap_{i=1}^{n_{k-2}} H_{\mathbf{y},\mathbf{w_i}}=0, H_{\mathbf{y},\mathbf{z}}=1, \right. \\
&\qquad \left. \bigcup_{i=1}^{n_{k-2}} H_{\mathbf{z},\mathbf{w_i}}=1, I^{k-1}_{\mathbf{z}}=1, \bigcap_{i=1}^{n_{k-2}} I^{k-2}_{\mathbf{w_i}}=1 \middle| \right. \\
&\qquad \left. N_{k-2}=n_{k-2} \right\}
\end{aligned}$$

$$\leq \sum_{j=1}^{n_{k-2}} \sum_{\mathbf{z}\in\mathbb{D}^d\setminus\{\mathbf{y},\mathbf{x_0}\}} \Pr\Bigg\{ J_{\mathbf{y}}=1, H_{\mathbf{y},\mathbf{w_j}}=0, H_{\mathbf{y},\mathbf{z}}=1, H_{\mathbf{z},\mathbf{w_j}}=1, I_{\mathbf{z}}^{k-1}=1, \bigcap_{i=1}^{n_{k-2}} I_{\mathbf{w_i}}^{k-2}=1 \Big| N_{k-2}=n_{k-2} \Bigg\} \quad \text{[union bound]}$$

$$= \sum_{j=1}^{n_{k-2}} \sum_{\mathbf{z}\in\mathbb{D}^d\setminus\{\mathbf{y},\mathbf{x_0}\}} \Bigg[\Pr\Big\{ J_{\mathbf{y}}=1, H_{\mathbf{y},\mathbf{w_j}}=0, H_{\mathbf{y},\mathbf{z}}=1 \Big| H_{\mathbf{z},\mathbf{w_j}}=1, I_{\mathbf{z}}^{k-1}=1, I_{\mathbf{w_j}}^{k-2}=1, N_{k-2}=n_{k-2} \Big\} \times \Pr\Bigg\{ H_{\mathbf{z},\mathbf{w_j}}=1, I_{\mathbf{z}}^{k-1}=1, \bigcap_{i=1}^{n_{k-2}} I_{\mathbf{w_i}}^{k-2}=1 \Big| N_{k-2}=n_{k-2} \Bigg\} \Bigg]. \tag{46}$$

Note that for any integer $1 \leq j \leq n_{k-2}$,

$$\sum_{\substack{\mathbf{w_1},\cdots,\mathbf{w_{j-1}},\mathbf{w_{j+1}},\cdots,\mathbf{w_{n_{k-2}}}\in\mathbb{D}^d\setminus\{\mathbf{y},\mathbf{x_0},\mathbf{z},\mathbf{w_j}\} \\ \mathbf{w_m}\neq\mathbf{w_n} \text{ for } m\neq n}} \Pr\Bigg\{ H_{\mathbf{z},\mathbf{w_j}}=1, I_{\mathbf{z}}^{k-1}=1, \bigcap_{i=1}^{n_{k-2}} I_{\mathbf{w_i}}^{k-2}=1 \Big| N_{k-2}=n_{k-2} \Bigg\}$$

$$= (n_{k-2}-1)! \Pr\Big\{ H_{\mathbf{z},\mathbf{w_j}}=1, I_{\mathbf{z}}^{k-1}=1, I_{\mathbf{w_j}}^{k-2}=1 \Big| N_{k-2}=n_{k-2} \Big\}. \tag{47}$$

Substitute Eq. (46) and (47) into Eq. (45),

$$\Pr\big\{ I_{\mathbf{y}}^{k}=1 \big| N_{k-2}=n_{k-2} \big\}$$

$$\leq \frac{1}{n_{k-2}!} \sum_{j=1}^{n_{k-2}} \sum_{\substack{\mathbf{z},\mathbf{w_j}\in\mathbb{D}^d\setminus\{\mathbf{y},\mathbf{x_0}\} \\ \mathbf{z}\neq\mathbf{w_j}}} \Big[\Pr\Big\{ J_{\mathbf{y}}=1, H_{\mathbf{y},\mathbf{w_j}}=0, H_{\mathbf{y},\mathbf{z}}=1 \Big| H_{\mathbf{z},\mathbf{w_j}}=1, I_{\mathbf{z}}^{k-1}=1, I_{\mathbf{w_j}}^{k-2}=1, N_{k-2}=n_{k-2} \Big\} \times (n_{k-2}-1)! \Pr\Big\{ H_{\mathbf{z},\mathbf{w_j}}=1, I_{\mathbf{z}}^{k-1}=1, I_{\mathbf{w_j}}^{k-2}=1 \Big| N_{k-2}=n_{k-2} \Big\} \Big]$$

$$= \sum_{\substack{\mathbf{z},\mathbf{w}\in\mathbb{D}^d\setminus\{\mathbf{y},\mathbf{x_0}\} \\ \mathbf{z}\neq\mathbf{w}}} \Big[\Pr\big\{ J_{\mathbf{y}}=1, H_{\mathbf{y},\mathbf{w}}=0, H_{\mathbf{y},\mathbf{z}}=1 \big| H_{\mathbf{z},\mathbf{w}}=1, I_{\mathbf{z}}^{k-1}=1, I_{\mathbf{w}}^{k-2}=1, N_{k-2}=n_{k-2} \big\} \times \Pr\big\{ H_{\mathbf{z},\mathbf{w}}=1, I_{\mathbf{z}}^{k-1}=1, I_{\mathbf{w}}^{k-2}=1 \big| N_{k-2}=n_{k-2} \big\} \Big]. \tag{48}$$

Since

$$\Pr\big\{ H_{\mathbf{z},\mathbf{w}}=1, I_{\mathbf{z}}^{k-1}=1, I_{\mathbf{w}}^{k-2}=1 \big| N_{k-2}=n_{k-2} \big\} = \frac{\Pr\big\{ H_{\mathbf{z},\mathbf{w}}=1, I_{\mathbf{z}}^{k-1}=1, I_{\mathbf{w}}^{k-2}=1, N_{k-2}=n_{k-2} \big\}}{\Pr\big\{ N_{k-2}=n_{k-2} \big\}} \tag{49}$$

and

$$\sum_{n_{k-2}=1}^{\infty} \Pr\big\{ H_{\mathbf{z},\mathbf{w}}=1, I_{\mathbf{z}}^{k-1}=1, I_{\mathbf{w}}^{k-2}=1, N_{k-2}=n_{k-2} \big\} = \Pr\big\{ H_{\mathbf{z},\mathbf{w}}=1, I_{\mathbf{z}}^{k-1}=1, I_{\mathbf{w}}^{k-2}=1 \big\}, \tag{50}$$

using Eq. (48), (49) and (50) we obtain

$$\Pr\big\{ I_{\mathbf{y}}^{k}=1 \big\}$$

$$= \sum_{n_{k-2}=1}^{\infty} \Big[\Pr\big\{ I_{\mathbf{y}}^{k}=1 \big| N_{k-2}=n_{k-2} \big\} \Pr\big\{ N_{k-2}=n_{k-2} \big\} \Big]$$

$$\leq \sum_{\substack{\mathbf{z},\mathbf{w}\in\mathbb{D}^d\setminus\{\mathbf{y},\mathbf{x_0}\} \\ \mathbf{z}\neq\mathbf{w}}} \Big[\Pr\big\{ J_{\mathbf{y}}=1, H_{\mathbf{y},\mathbf{w}}=0, H_{\mathbf{y},\mathbf{z}}=1 \big| H_{\mathbf{z},\mathbf{w}}=1, I_{\mathbf{z}}^{k-1}=1, I_{\mathbf{w}}^{k-2}=1 \big\} \times \Pr\big\{ H_{\mathbf{z},\mathbf{w}}=1, I_{\mathbf{z}}^{k-1}=1, I_{\mathbf{w}}^{k-2}=1 \big\} \Big]. \tag{51}$$

Hence we obtain Eq. (13).

REFERENCES

[1] P. Gupta and P. R. Kumar, "Critical power for asymptotic connectivity in wireless networks," *Stochastic Analysis, Control, Optimization and Applications: A Volume in Honor of W.H. Fleming*, W. M. McEneaney, G. Yin, and Q. Zhang, editors, pp. 547–566, 1998.

[2] ——, "The capacity of wireless networks," *IEEE Trans. Inf. Theory*, vol. 46, no. 2, pp. 388–404, 2000.

[3] M. Franceschetti, O. Dousse, D. N. C. Tse, and P. Thiran, "Closing the gap in the capacity of wireless networks via percolation theory," *IEEE Trans. Inf. Theory*, vol. 53, no. 3, pp. 1009–1018, 2007.

[4] O. Dousse, M. Franceschetti, and P. Thiran, "The costly path from percolation to full connectivity," in *Proc. 2004 Allerton Conference on Communication, Control and Computing*, pp. 893–903.

[5] ——, "On the throughput scaling of wireless relay networks," *IEEE Trans. Inf. Theory*, vol. 52, no. 6, pp. 2756–2761, 2006.

[6] P. Santi and D. M. Blough, "The critical transmitting range for connectivity in sparse wireless ad hoc networks," *IEEE Trans. Mobile Computing*, vol. 2, no. 1, pp. 25–39, 2003.

[7] X. Ta, G. Mao, and B. D. O. Anderson, "On the properties of giant component in wireless multi-hop networks," in *Proc. 2009 IEEE Conference on Computer Communications*, pp. 2556–2560.

[8] J. Li, L. L. Andrew, C. H. Foh, M. Zukerman, and H.-H. Chen, "Connectivity, coverage and placement in wireless sensor networks," *Sensors*, vol. 9, no. 10, pp. 7664–7693, 2009.

[9] R. Mulligan and H. M. Ammari, "Coverage in wireless sensor networks: a survey," *Network Protocols and Algorithms*, vol. 2, no. 2, pp. 27–53, 2010.

[10] B. Liu and D. Towsley, "A study of the coverage of large-scale sensor networks," in *Proc. 2004 IEEE International Conference on Mobile Ad-hoc and Sensor Systems*, pp. 475–483.

[11] H. M. Ammari and S. K. Das, "Critical density for coverage and connectivity in three-dimensional wireless sensor networks using continuum percolation," *IEEE Trans. Parallel Distrib. Systems*, vol. 20, no. 6, pp. 872–885, 2009.

[12] L. Booth, J. Bruck, M. Franceschetti, and R. Meester, "Covering algorithms, continuum percolation and the geometry of wireless networks," *The Annals of Applied Probability*, vol. 13, no. 2, pp. 722–741, 2003.

[13] S. Zhao, L. Fu, X. Wang, and Q. Zhang, "Fundamental relationship between node density and delay in wireless ad hoc networks with unreliable links," in *Proc. 2011 International Conference on Mobile Computing and Networking*, pp. 337–348.

[14] Z. Kong and E. M. Yeh, "On the latency for information dissemination in mobile wireless networks," in *Proc. 2008 ACM International Symposium on Mobile Ad Hoc Networking and Computing*, pp. 139–148.

[15] O. Dousse, P. Mannersalo, and P. Thiran, "Latency of wireless sensor networks with uncoordinated power saving mechanisms," in *Proc. 2004 ACM International Symposium on Mobile Ad Hoc Networking and Computing*, pp. 109–120.

[16] B. Liu, P. Thiran, and D. Towsley, "Capacity of a wireless ad hoc network with infrastructure," in *Proc. 2007 ACM International Symposium on Mobile Ad Hoc Networking and Computing*, pp. 239–246.

[17] R. Meester and R. Roy, *Continuum Percolation*. Cambridge University Press, 1996.

[18] M. Franceschetti and R. Meester, *Random Networks for Communication: From Statistical Physics to Information Systems*. Cambridge University Press, 2007.

[19] Z. Kong and E. M. Yeh, "Analytical lower bounds on the critical density in continuum percolation," in *Proc. 2007 International Symposium on Modeling and Optimization in Mobile, Ad Hoc and Wireless Networks and Workshops*, pp. 1–6.
[20] ——, "Connectivity and latency in large-scale wireless networks with unreliable links," in *Proc. 2008 IEEE Conference on Computer Communications*, pp. 394–402.
[21] M. Haenggi, J. G. Andrews, F. Baccelli, O. Dousse, and M. Franceschetti, "Stochastic geometry and random graphs for the analysis and design of wireless networks," *IEEE J. Sel. Areas Commun.*, vol. 27, no. 7, pp. 1029–1046, 2009.
[22] O. Dousse and P. Thiran, "Connectivity vs capacity in dense ad hoc networks," in *Proc. 2004 IEEE Conference on Computer Communications*, pp. 476–486.
[23] B. Bollobás and O. Riordan, *Percolation*. Cambridge University Press, 2006.
[24] S. C. Ng and G. Mao, "Analysis of k-hop connectivity probability in 2-D wireless networks with infrastructure support," in *Proc. 2010 IEEE Global Communications Conference*, pp. 1–5.
[25] T. S. Rappaport, *Wireless Communications: Principles and Practice*, 2nd edition. Prentice Hall PTR, 2002.
[26] A. Goldsmith, *Wireless Communications*. Cambridge University Press, 2005.
[27] T. K. Philips, S. S. Panwar, and A. N. Tantawi, "Connectivity properties of a packet radio network model," *IEEE Trans. Inf. Theory*, vol. 35, no. 5, pp. 1044–1047, 1989.
[28] B. Gu and X. Hong, "Critical phase of connectivity in wireless network expansion," in *Proc. 2010 IEEE Global Communications Conference*, pp. 1–5.
[29] Y. Li and Y. Yang, "Asymptotic connectivity of large-scale wireless networks with a log-normal shadowing model," in *Proc. 2010 IEEE Vehicular Technology Conference*, pp. 1–5.
[30] T. Yang, G. Mao, and W. Zhang, "Connectivity of wireless CSMA multi-hop networks," in *Proc. 2011 IEEE ICC*, pp. 1–5.
[31] M. Penrose, *Random Geometric Graphs*. Oxford University Press, 2003.
[32] J. Jachymski, "König chains for submultiplicative functions and infinite products of operators," *Trans. American Mathematical Society*, vol. 361, no. 11, pp. 5967–5981, 2009.
[33] S. Li, "Concise formulas for the area and volume of a hyperspherical cap," *Asian J. Mathematics & Statistics*, vol. 4, no. 1, pp. 66–70, 2011.
[34] T. Aste and D. Weaire, *The Pursuit of Perfect Packing*. Institute of Physics Publishing, 2000.
[35] J. H. Conway and N. J. A. Sloane, *Sphere Packings, Lattices and Groups*, 3rd edition. Springer, 1999.
[36] C. D. Lorenz, R. May, and R. M. Ziff, "Similarity of percolation thresholds on the HCP and FCC lattices," *J. Statistical Physics*, vol. 98, no. 3, pp. 961–970, 2000.

Seh Chun Ng received his BEng degree in Information Technology & Telecommunication from University of Adelaide, Australia, in 2000. He received his MSc degree in Information Technology from Malaysia University of Science and Technology (MUST), Malaysia in 2006 and Ph.D. degree in Engineering from University of Sydney in 2012. He was also with National ICT Australia (NICTA) during his Ph.D. study. His research interests is in wireless multi-hop networks, graph theory and queueing theory. He is currently a researcher in MIMOS, Malaysia.

Guoqiang Mao received the Bachelor degree in electrical engineering, the Master degree in engineering and PhD in telecommunications engineering in 1995, 1998 and 2002 from Hubei Polytechnic University, South East University and Edith Cowan University respectively. He joined the School of Electrical and Information Engineering, the University of Sydney in December 2002 where he is an Associate Professor now. He has published over one hundred papers in journals and refereed conference proceedings. He has served as a program committee member in a number of international conferences and an Associate Editor of the IEEE TRANSACTIONS ON VEHICULAR TECHNOLOGY. His research interests include intelligent transport systems and vehicular networks, wireless multihop networks, sensor networks, wireless localization techniques, cooperative communications, and graph theory and its application in networking. He is a Senior Member of IEEE.

Brian Anderson was born in Sydney, Australia, and received his undergraduate education at the University of Sydney, with majors in pure mathematics and electrical engineering. He subsequently obtained a PhD degree in electrical engineering from Stanford University. Following completion of his education, he worked in industry in Silicon Valley and served as a faculty member in the Department of Electrical Engineering at Stanford. He was Professor of Electrical Engineering at the University of Newcastle, Australia from 1967 until 1981 and is now a Distinguished Professor at the Australian National University and Distinguished Researcher in National ICT Australia Ltd. His interests are in control and signal processing. He is a Fellow of the IEEE, Royal Society London, Australian Academy of Science, Australian Academy of Technological Sciences and Engineering, Honorary Fellow of the Institution of Engineers, Australia, and Foreign Associate of the US National Academy of Engineering. He holds doctorates (honoris causa) from the Université Catholique de Louvain, Belgium, Swiss Federal Institute of Technology, Züich, Universities of Sydney, Melbourne, New South Wales and Newcastle. He served a term as President of the International Federation of Automatic Control from 1990 to 1993 and as President of the Australian Academy of Science between 1998 and 2002. His awards include the IEEE Control Systems Award of 1997, the IFAC Quazza Medal in 1999, the 2001 IEEE James H Mulligan, Jr Education Medal, and the Guillemin-Cauer Award, IEEE Circuits and Systems Society in 1992 and 2001, the Bode Prize of the IEEE Control System Society in 1992 and the Senior Prize of the IEEE TRANSACTIONS ON ACOUSTICS, SPEECH AND SIGNAL PROCESSING in 1986.